Journal of Engineering Physics and Thermophysics, Vol. 69, No. 1, 1996

DEVELOPMENT OF COMBINED METHODS OF HIGH-INTENSITY SURFACE TREATMENT. II. ELECTRIC AND ELECTRONIC TREATMENT

M. L. Kheifets, L. M. Kozhuro,
A. A. Shipko, and I. A. Senchilo

UDC 536.75:621.7:621.8:621.9

We investigated electrical and electronic methods of combined treatment of surfaces. Basic principles are formulated making it possible to control thermomechanical and electromagnetic effects, as well as concentrated energy fluxes when forming the properties of the surface layer of a workpiece.

1. Electromagnetic Facing with Surface Plastic Deformation. Electromagnetic facing with surface plastic deformation (SPD) is a technological process that combines the application, heat treatment, and deformation of coatings and reduces the running-in of the surface due to the formation of a rational geometry and structure of the surface layer (Fig. 1a). The thermomechanical processes in the combined method are governed by electromagnetic effects. The method is employed for strengthening and reclaiming the parts of machines using coatings made of ferromagnetic powders [1]. A finely dispersed structure and a partially amorphous state of the part are ensured by the initial conditions, i.e., rapid chilling of a thin molten layer of the coating applied. A rational geometry and strengthening of the surface are achieved by applying a deforming tool that changes the boundary conditions by additional rolling and rotating motions of a small ball.

1.1. Investigative Technique. First, on the basis of experimental data and using the P_z, P_y, and P_x components of the deforming force, as well as contact areas l and h, we determined the fields of stresses (Fig. 1c) in the surface layers of a workpiece restored by facing and in the coating strengthened by a ball roller.

For elastoplastic layers of the material treated we calculated the equivalent stresses σ_ε at variable elasticity parameters [2] by the method of successive approximations of elastic solutions [3]. Assuming in the initial approximation that $\chi = \chi_0$, we determined the regions in the deformed half-space with equivalent stresses σ_ε that exceeded those admissible in elastic deformations and further considered these regions at new values of the coefficient χ. The normal (σ_z, σ_y) and shear (τ_{zy}) stresses were calculated from the Airy stress functions [4].

Then, using the temperatures T of the contact areas and of the surface of the workpiece, we determined the temperature fields (Fig. 1b) in the surface layers of the restored part and in the coating.

And finally, using the results of calculations of the temperature fields and stress fields, we performed comparisons with the distributions over the depth H of the microstructures of the elements composing the surface layers (Fig. 2) and of the surface microhardness H_μ (Fig. 3) that had been obtained by x-ray structural analysis and scanning electron microscopy.

To determine the α-phase lattice period, we used extrapolation by the expression $0.5(\cos^2\Theta/\sin\Theta + \cos^2\Theta/\Theta)$ for all of the visible spectrum lines. The method is based on the existence of a linear dependence between the crystalline lattice period and the function $(\cos^2\Theta/\sin\Theta + \cos^2\Theta/\Theta)$ that is preserved at both large and small slip angles [5].

We calculated microstresses and the magnitude of the mosaic blocks using a standard procedure based on approximation of the lines of a standard and the investigated specimens [6]. As the standard, we used the original specimen and Armco iron.

Polotsk State University, Novopolotsk; Belarusian Agrarian Technical University, Minsk; Institute of Reliability and Longevity of Machines, Academy of Sciences of Belarus, Minsk; St.Petersburg State Technical University, Russia. Translated from Inzhenerno-Fizicheskii Zhurnal, Vol. 69, No. 1, pp. 43-54, January-February, 1996. Original article submitted September 21, 1994.

 1062-0125/96/6901-0036$15.00

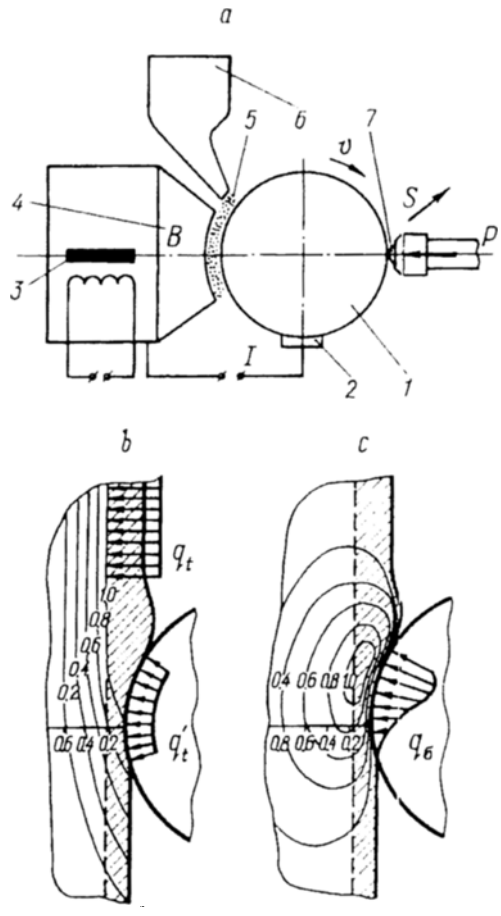

Fig. 1. Facing with surface plastic deformation (a): 1) treated workpiece; 2) sliding contact; 3) electric magnet; 4) pole tip; 5) ferric powder; 6) batcher; 7) ball roller; thermal field (1.0 corresponds to 1000 K) (b) and stress field (1.0 corresponds to 1000 MPa) (c) in the zone of surface formation (dimensions are given in mm).

We estimated the lumpiness of the structure by the front line, approximating it by the function $y_0/(1 + 6x^2)$, and the stresses by the rear line of the α-phase, approximating it by the function $y_0/(1 + 8x^2)^2$.

We determined the carbon content of the martensite by the position of the (101) line (the second line of the (110) doublet is superimposed on the α – Fe line obtained for untreated portions of the specimen surface falling within the x-ray view) and calculated it using a quadratic formula for a tetragonal system and Kurdyumov's procedure for determining the interplanar spaces in martensite [7].

We determined the dislocation density from the results of the x-ray analysis from the physical broadening of the interference lines with a small sum of the squares of the indices, in particular, using the (211) β line. We calculated the dislocation density from the formula obtained in [5]:

$$\rho = \beta^2 k/(FB^2) .$$

1.2. Results and Discussion. The stress fields and temperature in the surface layers calculated from experimental data for a workpiece restored by facing and for a coating strengthened by a ball roller (Fig. 1) show that combining highly intense thermal and deformational effects in the process of surface strengthening should cause specific changes in the kinetics of plastic deformation, while in the surface layer of the workpiece, both in the coating and beyond it, strengthening structures may be formed at a depth of 0.2–0.3 mm.

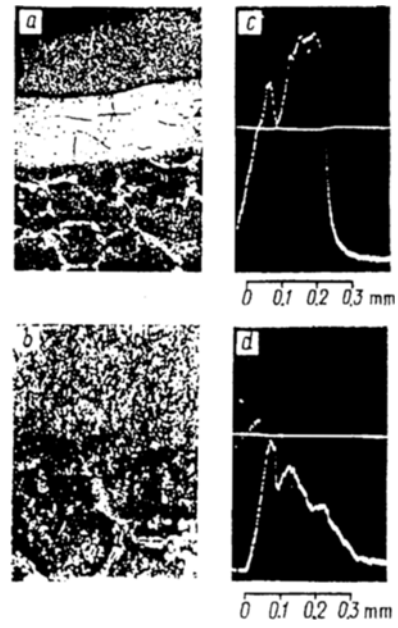

Fig. 2. Microstructures of electromagnetical facing of S-300 high-chromium powder (a) and steel powder with additions of vanadium FeV with subsequent surface plastic deformation (b); distributions of chromium over the depth of facing with S-300 powder (c) and of vanadium on facing with FeV powder (d) (×300).

When coatings are applied by electromagnetic facing, the ferropowder particles are aligned in a magnetic field as electrode chains and, as a result of electric arc discharges, are deposited onto the surface treated. Electromagnetic facing makes it possible to apply a coat only of a certain thickness, after which the coating layer loses stability, and peaks are formed on the surface that become craters after subsequent discharges [8]. The facing process can be controlled by electromagnetic fluxes, which, in addition to fixing the ferropowder particles, ensure intense heat release at the places of their contact with the surface formed, i.e., by changing the electric resistance of the deposited layer, they regulate its thickness [1].

When applying coatings, a strengthened layer consisting of the material powder and outer portion of the backing is formed on the surface of the workpiece; the strengthening occurs due to heating with subsequent rapid chilling and to diffusion of the coating elements (Fig. 2a). In the strengthened layer we can isolate two sequentially positioned zones with different structures and phase compositions: the coating itself, which involves a portion of the workpiece after heating by contact with the liquid metal of the coating and rapid chilling by heat removal to the backing, and a transition zone, which plays an important role in the subsequent use of the workpiece.

The exterior part of a facing layer, irrespective of the composition of the powder used, is an agglomeration of very fine metallic plates, which by state represent a supersaturated solid solution of the powder components in α- or γ-iron. We did not discover carbide particles in any of the coatings investigated. A surface layer produced by facing (without subsequent SPD) is distinguished by a rather distinct boundary between the coating and the steel 45 backing. This is especially apparent for a facing of S-300 high-chromium iron (Fig. 2a). At the same time great changes are observed in the structure of the thermal effect, whose depth exceeds that of the facing layer. As a result of the diffusion of carbon into the austenite that was formed by the temperature increase at the boundary with the superheated melt of the powder and subsequent rapid chilling, a weakly etching dislocation martensite is formed whose hardness somewhat exceeds that of the facing layer.

Investigation of the distribution of chromium over the depth of facing layer of S-300 powder and of the topography of the surface in chromium emission (Fig. 2c) shows that all of the chromium is concentrated in the facing layer; it is not volatilized while being deposited and does not diffuse into the backing. The distribution of chromium in the layer is uniform due to the formation of a homogeneous solid solution during facing. The peaks

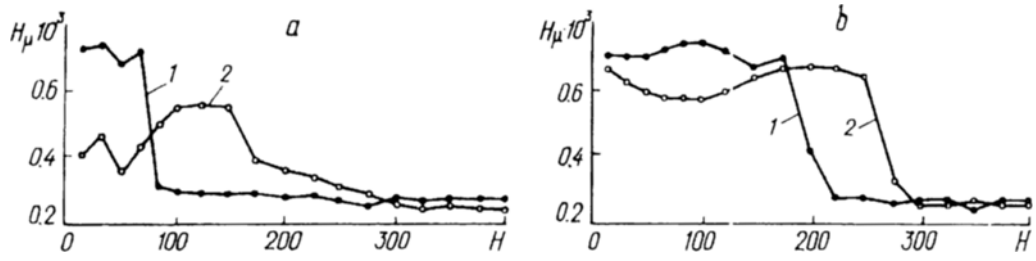

Fig. 3. Dependences of the change in the microhardness H_μ (MPa) over the surface layer depth H (μm) on electromagnetic facing (1) and subsequent surface plastic deformation (2) of coatings of steel powder FeV with additions of vanadium and of powder of R6M5F3 high-speed steel (b).

on the curve are attributed to the superposition of successive steps of electromagnetic deposition. The absence of chromium in the transition layer confirms the presence of a sharp boundary between the facing and the backing. The same picture is characteristic a facing without SPD for other coatings.

When the facing is deformed, additional degrees of freedom allow the smoothing ball, in addition to rolling, to perform spinning as a result of interaction with the protrusions on the surface being treated [9]. Without additional heating the degree of deformation is not large, while the trajectory of the ball is a loop. When heated, the material treated is more plastic as a result of which the degree of deformation and the frictional drag coefficient increase. This impedes the spinning and reduces the length of the ball trajectory, thus decreasing the intensity of deformation processes. As a result, the heating of the surface and additional spinning of the ball make it possible to control the process of deformation in electromagnetic facing.

A study of the structures of surface layers after facing with R6M5F3 high-speed steel powder and steel powder with added vanadium, Fe + 10% V, with SPD (Fig. 2b) reveals the following specific features: the density and homogeneity of the exterior portion of the facing are higher; the boundaries between the deposited layer and the backing are more highly blurred; the diffusion layer, in which conversions occur that correspond to full hardening, is more developed; the zone of thermal effect is deeper and phase conversions in it are developed more fully; the change in microhardness with transition from the facing to the backing is smoother.

Let us consider the zone of thermal effect, in which we can distinguish several regions. At the boundary between a facing and a backing of steel 45 there is a region of full hardening that consists of acicular martensite. It adjoins a region of incomplete hardening consisting of martensite, troostite, and ferrite. In the ferrite we observe fragmentation of the grains as a result of recrystallization caused by heating and deformation. This is indicative of the effect of the SPD not only on the facing but also on the surface layers of the backing.

The occurrence of diffusion processes in the transition layer is also evidenced by the character of the distribution of alloying elements contained in the powder. The character of the distribution of vanadium in the surface layer of the specimen with a facing of Fe +10% V and with SPD (Fig. 2d) shows that the concentration of V attains a maximum in the facing but then smoothly decreases in the direction of the backing. That diffusion processes in facing with SPD occur at larger depths is also indicated by the distribution of microhardness over the surface layer depth (Fig. 3), which is nonmonotonic. The minimum and maximum microhardness are observed near the boundary between the facing and backing, which is associated with the redistribution of carbon because of increased solubility in the liquid phase and decarburization at the liquid-solid phase interface.

The total depth of hardening of a facing with SPD is 0.15–0.25 mm (Fig. 3, curve 2), while without SPD it is 0.10–0.15 mm (Fig. 3, curve 1).

X-ray diffraction analysis makes it possible to evaluate the level of microstresses, the dispersity of the structure, and content of carbon in solid solution and to characterize the dislocation structure and identify the phases contained in the structure of the coating.

X-ray diffraction analysis of the R6M5F3 powder coating (without SPD) reveals two types of oversaturated solid solutions: with bcc (martensite) and fcc (austenite) lattices. The computed results of the *x*-ray records of coatings for the (110) lines show their shift to the side of smaller angles, which is associated with an increase in

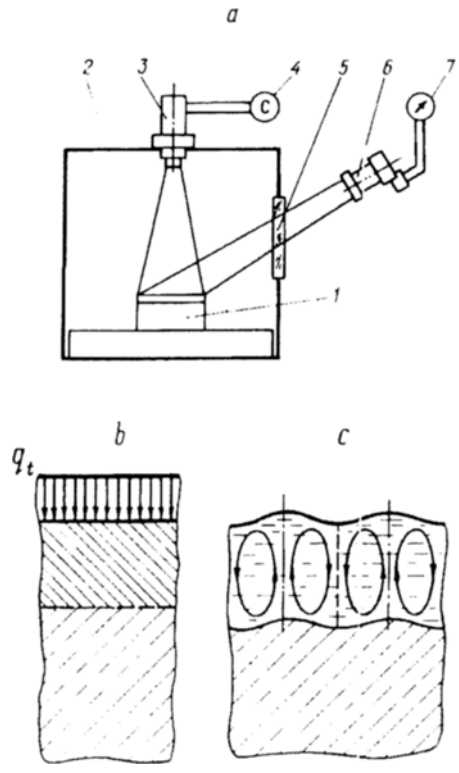

Fig. 4. Electron-beam heating of coated surface (a): 1) treated workpiece; 2) vacuum chamber; 3) electron gun, systems of focusing and scanning; 4) stopwatch; 5) illuminator; 6) pyrometer; 7) millivoltmeter; fusion of coated surface (b); and thermocapillary convection in a liquid phase with fusion (c).

the density of defects introduced into the α-solid solution structure. The lines of the solid solution of the R6M5F3 coatings with SPD have a maximum shift. In R6M5F3 powder coatings with SPD, austenite is absent, since it decomposes under plastic deformation.

Virtually all the carbon in R6M5F3 coatings is in solid solution. In a S-300 coating only 0.98% of carbon is contained in the martensite, a portion is incorporated into the austenite, and a portion enters into the composition of extremely dispersed eutectic chromium and vanadium carbides.

The calculated data on the dimensions of the blocks of coherent scattering and density of dislocations show that SPD increases the density of the defects introduced into the structure of the martensite and decreases the dimensions of the blocks of coherent scattering.

An approximate evaluation of the level of microstresses shows that they are smaller than in other methods of applying coatings. This positively characterizes the combined method.

The line-diagrams of the x-ray records of workpieces with S-300 and R6M5F3 powder coatings (considered after SPD and additional triple tempering at 500°C) and the data on the distribution of microhardness over the hardened layer depth show that additional tempering leads to the evolution of a large quantity of special highly dispersed carbides and to a substantial increase in hardness. The carbides are arranged both along the boundaries and in the interior of the grains of the former austenite.

The formation of texture in the surface layer in electromagnetic facing, the increased density of crystalline structure defects, the formation of dispersed uniformly distributed carbides in the case of SPD, and additional tempering improve the performance characteristics of the hardened parts of machines.

Conclusions

1. A change in the initial and boundary conditions of thermomechanical processes in the application of coatings and their surface plastic deformation can occur when energy fluxes of a different nature are used, such as magnetic for moving and fixing applied particles and electric for heating and melting the particles.

2. Technological-service barriers formed by electromagnetic, thermomechanical, or other energy fluxes interact with the existing barriers, which were formed by various substance fluxes; they are dissipated by the latter barriers or absorb them.

3. Inherited structures may be preserved and may influence the formation and service life of surfaces or may change and decompose, absorbing an appreciable quantity of energy in a relatively short period of time by spatially restricted layers.

2. Electron-Beam Heating of a Coated Surface. The electron-beam heating of a surface having a galvanic, chemical, or a detonation-applied coating is a technological process that combines the application of a coating and the melting of the coating itself and its backing with the formation of a diffusional transition layer of large thickness (Fig. 4a). Depending on the regime of thermal treatment, thickness, and composition of the coating, the melted layer may have a fine-block or a cellular structure [10, 11]. The formation of the structure is governed by the initial conditions, i.e., melting at a high rate and rapid chilling of the molten layer, and also by the boundary conditions, such as the trajectory and velocity of the electron beam.

2.1. Investigative Technique. First, on the basis of the obtained experimental data on the temperatures T on the surface of the heated workpiece we determined the temperature fields in the surface layers treated by an electron beam. Then, we compared the results of calculations of the temperature fields with the results obtained by x-ray diffraction analysis and electron microscopy for the distributions, over the depth H of the microstructures (Fig. 5), of the phase and elemental composition, as well as of the microhardness H_μ (Fig. 6) of the surface layers.

The data of the x-ray diffraction analysis and scanning electron microscopy were processed by the techniques considered in [12-15].

2.2. Results and Discussion. The electron beam heating of workpieces made of VT6 and VT9 titanium alloys with the visible portion of the hardened layer up to 1.3 mm thick increases the dimensions of the β-converted grain over a cross-section of the treated surfaces up to 150 μm. In this case, the dimension of the martensite plates is determined not only by the diameter of the grain, but also by the structural microinhomogeneity appearing because of the retardation of diffusion processes in electron-beam heating and due to high cooling rates. Near the surface of the workpieces that were subjected to heating, the phase composition is determined by the presence of two types of martensite, α' and α'', with a variable concentration of β-stabilizing alloying elements. This is associated with the wide spectrum of concentrations in the structure on dissolution of the α-phase at the moment of $\alpha - \beta$-conversion under conditions of rapid heating. The hardness gradually decreases in this case from 43–45 HRC_e on the surface to 24–37 HRC_e in the material of the base.

The distribution of aluminum and titanium makes it possible to isolate two surface layers. In the first layer, at a depth of 140–160 μm, their homogeneous distribution is observed, with the aluminum concentration being about two times smaller than in the initial alloy. In the second layer, an increased content of aluminum and decreased content of titanium were discovered. With distance from the surface, the structure of the alloy retains a large quantity of the α-phase, and also of portions of the β-solid solution with a reduced concentration of molybdenum that were formed under conditions of rapid heating during dissolution of the α-phase particles. Consequently, the difference between the concentrations of the alloy components in microvolumes increases on moving away from the surface. If we take into account the fact that the α-phase, as well as the portions of the β-phase with a reduced content of molybdenum, have an increased concentration of aluminum, we may assume that the process of electron-beam heating causes the directed motion of aluminum atoms into the zones with the smallest concentration. Corresponding to them are the volumes of the β-phase bordering on undissolved particles and zones of reduced concentration of molybdenum and located in the portions of the solid solution that are more removed from the surface. With a rise in the heating temperature, the surface portions of the β-solid solution strive to achieve an equilibrium state, while the undissolved α-phase and the zones with a concentration difference move farther from the surface, and the concentrational conditions of the process alter.

In the case of electron-beam fusion (Fig. 4b) of the surfaces of the workpieces made of titanium alloys, thermocapillary convection (Fig. 4c) attributable to the dependence of the surface tension on the appreciable change in temperature causes the formation of the cells of hexagonal-cylindrical shape over the entire treated surface in the section of electron beam craters in the direction of the gravity force [10, 11]. The microstructure of the VT6

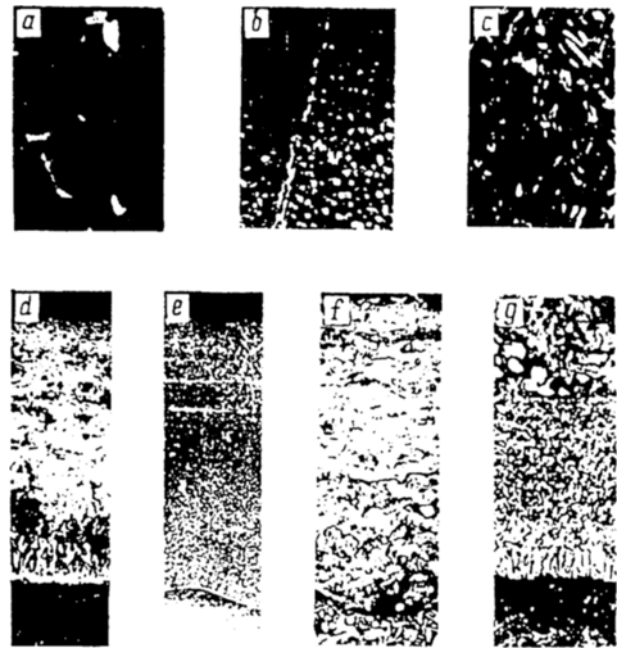

Fig. 5. Cellular structures on VT20 titanium alloy with unetched surface at the epicenter of heating (a), in transition region (b) and with an etched surface (c); microstructures of detonation-applied coatings of WC + 15%Ni (d, e) and WC + 25%Co (f, g) on VT9 titanium alloy in the initial state (d, f) and after electron heating (e, g) (×300).

and VT20 alloys after tempering from a liquid state is represented by rather densely packed cells with a diameter of 5–7 μm. Micropores at the joints of several grains have the diameter of up to 1 μm (Fig. 5a). In the zone of transition from the cellular to the β-transformed structure, the number and dimension of the cells decrease steadily, and the the grain size is equal to 100–200 μm (Fig. 5b). In the internal structure the maximum dimension of the martensite-type needles corresponds to the diameter of a cell (Fig. 5c). The distortion of the hexagonal shape of the cells increases with an increase in the alloying nature of the melt. For this reason the boundaries of the former β-grains are also partially retained on portions of the cellular structure.

In the process of the formation of dissipative structures, an intense redistribution of the alloying components occurs in the liquid phase; near the walls and at the corners of the cells, components are accumulated that reduce the surface tension. An intense concentrational stratification of the β-phase is indicated by the appearance of an alloyed α''-martensite in the VT20 single-phase pseudo-α-alloy in the regions with a cellular structure. The parameters of the $\alpha(\alpha')$-phase structure change from $a = 2.922$, $c = 4.667$ in the initial state to $a = 2.923$, $c = 4.729$ for the cellular structure, i.e., the tetragonality of the α'-martensite increases. The parameters of the α'-martensite are the following: $a = 2.952$, $b = 5.294$; $c = 4.691$. With the formation of the martensite-type α''-phase in the structure of the VT20 alloy the possibility of thermal hardening of the latter appears.

The electron-beam heating of oxidized surfaces of VT6 and VT23 alloys makes it possible to increase the microhardness both within the limits of the diffusion layer and under it, testifying to the motion of oxygen to deeper layers. This increases the thickness of the alphatized layer four times. The electron-beam heating of VT6 and VT23 alloys after siliconizing causes redistribution of the aluminum farther from the surface. The former alphatized layer increases by a factor of two, becomes more porous, and partially experiences martensite conversion. The total thickness and porosity of the layer of silicides also increase.

When a VT20 alloy with a stock galvanic chromium coating is exposed to heating by an electron beam, a structure with a grain diameter of 10–20 μm is formed. Then the thicknesses of the diffusion layer and of the residual coating are equal to 10–12 and 5–6 μm, respectively. The maximum value of the chromium grain is 3–5 times higher than the thickness of the coating itself. This effect can be explained by the presence of a boundary

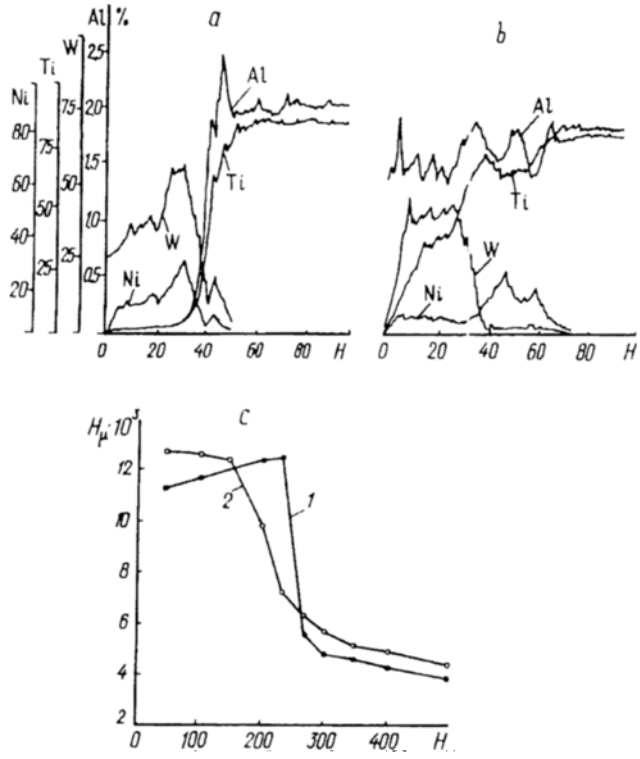

Fig. 6. Distribution of chemical elements of detonation-applied coating of WC + 15% Ni on VT9 titanium alloy in the initial state (a) and after electron beam heating (b); dependences of the change in the microhardness H_μ over the depth of the surface layer H in the initial state (1) and after electron-beam heating (2) of detonation-applied coating of WC + 25% Co on VT9 titanium alloy (c).

between the coating and the diffusion zone and by the influence of thermal etching during treatment in vacuum. As the temperature of heating increases, the continuity of the chromium coating is destroyed. Due to the higher intensity of the processes of boundary diffusion, the chromium diffuses along the boundaries of the β-grains of titanium into the titanium matrix of the VT20 alloy. In this case, the grain size of the backing is 80–120 μm. As the heating continues, melting of the $TiCr_2$ metallide begins with the formation of a characteristic fine-block structure with crystallization. The size of the blocks is equal to 2–10 μm, and the thickness of the diffusion layer is about 30 μm. As regards the regimes of diffusion saturation, electron-beam heating ensures the existence of alloying elements in the surface layers of the solid solution in α-titanium and $TiCr_2$ compound. The presence of α–Ti over virtually the entire diffusion layer thickness indicates to a larger amount of titanium in the layer than of chromium, which is completely bound with α–Ti in $TiCr_2$. Below in the section, where the concentration of chromium is insufficient for the formation of $TiCr_2$, chromium forms a β-solid solution with titanium.

In the case of electron-beam heating of a workpiece made of VT20 alloy, the grain structure of the original nickel coating is violated. After the increase in the temperature of heating, as a result of the recrystallization of the surface zone, the structure consists of equiaxial grains 10–30 μm in diameter with a well-characterized martensite intragranular structure. Martensite based on solid solutions and a β-solid solution of nickel in titanium are formed in the layers more removed from the surface. The formation of distinct grain boundaries is caused by the preferential diffusion of nickel along the boundaries of the β-grains of the VT20 alloy with the formation of metallic compounds. After a sharp increase in the intensity of heating we do not observe a layer-by-layer separation of metallides over the layer thickness due to the appearance of convection flows in the liquid phase.

In the case of electron-beam heating of a chromium coating with a backing of nickel on VT20 titanium alloy, the mutual formation of solid solutions occurs in the Ti–Ni–Cr system. Chromium passes into solid solution

with nickel, and a eutectic reaction with the formation of a liquid phase on the basis of Ti_2Ni occurs at the boundary between the nickel sublayer and titanium backing. The eutectic layer is crystallized in the form of dendrites with a length of 8–12 μm normal to the interface. With a further rise in temperature, the diffusion layer thickness attains 300–600 μm. With the development of eutectic reactions, convection flows appear in the molten pool that accelerate the exchange by elements between the coating and backing, and this leads to an increase in the growth of hardened layers and to the homogenezation of the diffusion zone.

Electron-beam heating of the surface of VT9 alloy with a detonation-applied coating on the basis of WC + 15% Ni leads to separation of the coating and of the adjoining layer of the backing into a number of characteristic zones (Figs. 5d and 5e). Due to the diffusion of nickel from the inner layers of the coating to the titanium, a zone of a solid solution of Ni in Ti is formed, and above it, interrelated zones of the eutectic β + Ti_2Ni and metallide Ti_2Ni, in which the concentration of Ni increases substantially (Figs. 6a and 6b). The total thickness of these zones is equal to about 20 μm. Together with the nickel, up to 5% of the W that forms a solid solution in the titanium diffuses into the titanium backing. The titanium concentration decreases smoothly in the direction of the surface, and that of the nickel remains approximately the same. In the process of heating, aluminum diffuses actively through the coating to the surface. An increase in the heating temperature causes conversion of the complex structure of the entire volume of the coating into a mixture of the eutectic with particles of tungsten carbide of round shape (Fig. 5e). After such treatment the surface of the coating acquires a fine-block structure with a block size of up to 1 μm.

When a coating based on WC + 25% Co is exposed to electron-beam heating, metal-bound compounds of titanium are formed at the interface with the backing (Figs. 5f and 5g). The appearance of a liquid phase sharply intensifies the diffusion processes. The thickness of the converted layer, in which the role of the binder is played by the eutectic based on $TiCO_2$, exceeds the thickness of the metallide layers in the titanium backing by a factor of 4–15 (Fig. 5h). This is associated with a higher rate of titanium diffusion in the metal-binder, as well as with a positive temperature gradient in the direction of titanium diffusion. The main distribution of the character of microhardness over an alloy section with a detonation-applied coating is associated with the creation of a smooth transition between the solid coating and titanium backing (Fig. 6c). The hardness of the 0.1–0.15 mm-thick surface layer after electron beam heating is preserved at the level of the original solid alloy with the hardness of the inner portion of the coating lower and the hardness of the titanium backing higher.

As we see, with electron beam heating of detonation-applied coatings the character of conversions and the phase composition are mainly determined by diffusion processes at the coating-backing interface. In contrast to heating of electrolytic coatings, in detonation-applied coatings the lamellar structure with a different content of chemical elements in layers is preserved up to 1500–1600°C. The tungsten carbide particles that were not fused in the process of heating prevent convective mixing in the zone of heating and, consequently, equalization of the concentrational and structural inhomogeneity.

Conclusions

1. The initial and boundary conditions connect the sequence of technological transitions in surface treatment and allow one to consider the evolution of a technological system from the energy and substance source through the processes of formation of the surface layers to the structures and phases formed in them.

2. Technological barriers isolate nonequilibrium systems from the surrounding effects and thus make possible the formation of nonequilibrium structures, cells, and phases whose creation is inattainable in an equlibrium state.

3. The structures and phases that form in nonequilibrium processes make of possible to inherit dissipative properties at all the stages of surface formation. Thus, the structural and geometric features of cells ensure phase-chemical inhomogeneities of surface layers.

NOTATION

S, rate of supply; v, velocity of main motion; I, current; B, magnetic induction; P, deforming force; P_z, P_y, and P_x, components of deforming force; T, temperature; l and h, lengths of contact areas; σ_e, equivalent stresses;

χ, coefficient in universial hardness tests; x, y, and z, coordinates of the current point; σ_z and σ_y, normal stresses; τ_{zy}, shear stresses; q_t and q_σ, power densities of the sources of thermal and deformational effects; HRC_e, surface hardness according to Rockwell; H_μ, microhardness of surface; H, depth of hardened layer; θ, angle of slip; ρ, density of dislocations; β, broadening of line; k, coefficient depending on the elastic and shear moduli; F, factor depending on the change in the elastic energy of a single dislocation on interaction with the stress field in a crystal; B, the Burgers vector; a, b, and c, crystal-lattice parameters.

REFERENCES

1. P. I. Yashcheritsyn, G. A. Deev, L. M. Kozhuro, and M. L. Kheifets, Dokl. Akad. Nauk Belarusi, 37, No. 4, 114-117 (1993).
2. A. V. Aleksandrov and V. D. Potapov, Fundamentals of the Theory of Elasticity and Plasticity [in Russian], Moscow (1990).
3. A. A. Il'yushin, Plasticity. Foundations of General Mathematical Theory [in Russian], Moscow (1963).
4. H. Han, Theory of Elasticity. Foundations of Linear Theory and Its Application [in Russian], Moscow (1988).
5. M. A. Krivoglaz, Theory of Scattering of X-Rays and Thermal Neutrons by Real Crystals [in Russian], Moscow (1967).
6. A. D. Vishnyakov, Present-Day Methods of Investigation of the Structure of Deformed Crystals [in Russian], Moscow (1975).
7. G. V. Kurdyumov, L. M. Utevskii, and R. I. Entin, Conversions in Iron and Steel [in Russian], Moscow (1977).
8. P. I. Yashcheritsyn, M. T. Zabavskii, L. M. Kozhuro, and L. M. Akulovich, Diamond-Abrasive Treatment and Hardening of Workpieces in a Magnetic Field [in Russian], Minsk (1988).
9. C. L. Jonson, Mechanics of Contact Interaction [Russian translation], Moscow (1989).
10. S. A. Astapchik, G. L. Tsarev, N. A. Bereza, and I. S. Chebot'ko, Izv. Akad. Nauk BSSR, Ser. Fiz.-Tekh. Nauk, No. 2, 13-18 (1987).
11. A. A. Shipko, Metalloved. Termich. Obrab. Metallov, No. 10, 45-49 (1987).
12. A. A. Shipko, I. L. Pobol', G. E. Gorelik, and A. E. Korolyov, Izv. Akad. Nauk BSSR, Ser. Fiz.-Tekh. Nauk, No. 1, 24-28 (1985).
13. A. A. Shipko and V. A. Zhurin, in: Problems of Treatment of Materials and Alloys [in Russian], Minsk (1975), pp. 94-95.
14. V. D. Kal'ner and A. G. Zimberman, Practice of Microprobe Methods for Investigating Metals and Alloys [in Russian], Moscow (1981).
15. L. I. Pushinskii and A. P. Plokhov, Investigation of the Structure and Physicomechanical Properties of Coatings [in Russian], Novosibirsk (1986).